frontiers | Frontiers in Genetics

TYPE Original Research
PUBLISHED 04 January 2023
DOI 10.3389/fgene.2022.1087201

OPEN ACCESS

EDITED BY
Wei Xu,
Shanghai Changzheng Hospital, China

REVIEWED BY
Hua Huang,
Tianjin Medical University, China
Jianyuan Chai,
Baotou Medical College, China

*CORRESPONDENCE
Qian Li,
liqian0816@sina.com

SPECIALTY SECTION
This article was submitted to Cancer Genetics and Oncogenomics, a section of the journal Frontiers in Genetics

RECEIVED 02 November 2022
ACCEPTED 02 December 2022
PUBLISHED 04 January 2023

CITATION
Zhao Z, Li C, Peng Y, Liu R and Li Q (2023), Construction of an original anoikis-related prognostic model closely related to immune infiltration in gastric cancer.
Front. Genet. 13:1087201.
doi: 10.3389/fgene.2022.1087201

Construction of an original anoikis-related prognostic model closely related to immune infiltration in gastric cancer

Zhihong Zhao, Cun Li, Ye Peng, Rui Liu and Qian Li*

Department of Gastroenterology, Xiangya Hospital Central South University, Changsha, China

Background: Anoikis is considered as a particular type of programmed cell death, the weakness or resistance of which contributes greatly to the development and progression of most malignant solid tumors. However, the latent impact of anoikis-related genes (ARGs) on gastric cancer (GC) is still ambiguous. Based on these, this study established an anoikis-related prognostic model of GC to identify the prognosis of patients and provide more effective treatment in clinical practice.

Methods: First, we extracted four public datasets containing the gene expression and clinicopathological information of GC, which were worked as the training and validating sets, separately. Then, an anoikis-related survival-predicted model of GC was developed *via* Lasso and COX regression analyses and verified by using the Kaplan-Meier (KM) curve and receiver operating characteristic (ROC) curve analyses. Next, we assigned GC patients to two groups characterized by the risk score calculated and analyzed somatic mutation, functional pathways, and immune infiltration between the different two groups. Finally, a unique nomogram was offered to clinicians to forecast the personal survival probability of GC patients.

Results: Based on seven anoikis-related markers screened and identified, a carcinogenic model of risk score was produced. Patients placed in the high-score group suffered significantly worse overall survival (OS) in four cohorts. Additionally, the model revealed a high sensitivity and specificity to prognosticate the prognoses of GC patients [area under the ROC curve (AUC) at 5-year = 0.713; GSE84437, AUC at 5-year = 0.639; GSE15459, AUC at 5-year = 0.672; GSE62254, AUC at 5-year = 0.616]. Apart from the excellent predictive performance, the model was also identified as an independent prediction factor from other clinicopathological characteristics. Combining anoikis-related prognostic model with GC clinical features, we built a more comprehensive nomogram to foresee the likelihood of survival of GC patients in a given year, showing a well-accurate prediction performance.

Conclusion: In summary, this study created a new anoikis-related signature for GC, which has potentially provided new critical insights into survival prediction and individualized therapy development.

KEYWORDS

gastric cancer, anoikis-related genes, prediction, prognosis, immune infiltration

Introduction

Statistically, gastric cancer (GC) ranks fifth in morbidity and fourth in mortality in all malignant solid tumors in the whole world (Sung et al., 2021). Though the rapid advancement of endoscopic technology facilitates the early diagnosis of GC, the prognosis of patients has not significantly improved, owing to the non-specific symptoms and notorious aggressiveness of GC (Krejs, 2010; Li et al., 2022a; He et al., 2022). The vast majority of death from cancer is not due to a primary tumor but a sequel of metastatic cells within the tumor disorder (Sethi and Kang, 2011; Adeshakin et al., 2021). Consequently, identifying effectual metastasis-related prognostic biomarkers is vital to early intervention and prognosis prediction of GC.

Anoikis, a particular form of apoptosis, is stimulated by the absence of the attachment between cells or between cells and nearby extracellular matrix (Frisch and Francis, 1994; Paoli et al., 2013). It prevents dysplastic cells, pre-cancerous epithelial cells, from departing from their primary location and spreading elsewhere, avoiding the aggressive behavior of the detached tumor cells (Taddei et al., 2012). Anoikis resistance, which is the breakdown or avoidance of anoikis, is expected to confer selective superiority upon the detached cancer cells, affording them an increased anchorage-independent survival time, thereby facilitating eventual reattachment and uncontrolled growth of other sites (Frisch and Screaton, 2001; Guadamillas et al., 2011; Khan et al., 2022). Anoikis is envisioned as a pivotal defense in combating tumor metastasis and maintaining normal tissue homeostasis (Kim et al., 2012; Paoli et al., 2013). However, few studies have evaluated anoikis-related signatures in GC.

Thus, in this study, we concentrated on the predictive performance of anoikis-related genes (ARGs) in the prognosis of GC and developed an anoikis-related risk score model. We further explored and compared the differences in the genetic mutation, functional enrichment, and immune microenvironment between the two risk groups.

Materials and methods

Data acquisition and preprocessing

The RNA-sequencing and relevant clinical information data of GC patients used as a training set were downloaded from The Cancer Genome Atlas (TCGA) database (https://portal.gdc.cancer.gov/). All of the raw counts were transformed to transcripts per million (TPM) and log2-modified before analysis. For validation, three microarray datasets (GSE84437, GSE15459, GSE62254) along with related clinical data were acquired from Gene Expression Omnibus (GEO) database (https://www.ncbi.nlm.nih.gov/geo/) and easyGEO database (https://easygeo.cn/). The raw data of GSE84437 were quantile normalized and log2-modified before analysis. After removing duplication, 740 ARGs were integrated from the GeneCards database (https://www.genecards.org/), Harmonizome database (https://maayanlab.cloud/Harmonizome/), and National Center for Biotechnology Information (NCBI) database (https://www.ncbi.nlm.nih.gov/) (Supplementary Table S1) (Rouillard et al., 2016).

Identification of anoikis-related prognostic markers

First, we intersected the gene symbols from TCGA-STAD and GSE84437 cohorts to guarantee that the genes achieved from the following analysis were shared and removed the batch effect between the data of two datasets by operating the "sva" R package to ensure the comparability. Then, the "limma" R package was utilized to analyze the genes with differences in expression between tumor and adjacent normal tissues in the TCGA cohort (Ritchie et al., 2015). Setting the criteria of absolute fold change ($|logFC| > 1.0$ and adjusted p-value <0.05, we selected 1,482 differentially expressed genes (DEGs). Further, taking the intersection of ARGs and DEGs, extracting the expression matrix of intersectant genes, and combining the matched survival information, univariable Cox regression analysis was performed on TCGA-STAD and GSE84437 cohorts separately to pick out potential genes affecting the outcome of GC patients ($p < 0.05$). The Venn diagram was depicted to show the intersectant genes *via* the "VennDiagram" R package.

Functional enrichment analysis

Based on anoikis-related DEGs, Gene Ontology (GO), Kyoto Encyclopedia of Genes and Genomes (KEGG), and Gene Set Enrichment Analysis (GSEA) enrichment analyses were conducted to seek out underlying functional pathway, by using multiple R packages ("clusterProfiler", "enrichplot", and "ggplot2") (Kanehisa and Goto, 2000; Subramanian et al., 2005; Kanehisa et al., 2021). Two gene sets ("c2.cp.kegg.v2022.1.Hs.symbols.gmt", "h.all.v2022.1.Hs.symbols.gmt") were collected from the Molecular Signatures Database (https://www.gsea-msigdb.org/gsea/msigdb) for GSEA analysis (Subramanian et al., 2005).

Risk score calculation

The TCGA-STAD data were worked as the training set as noted before. We made use of The Least Absolute Shrinkage and Selection Operator (LASSO) Cox regression technology to identify the promising prognostic markers and produce the anoikis-related gene prognostic score (ARGPS) model. The expression level of the candidate genes and the corresponding

regression coefficients were employed as the key components of the models. The formula for calculating ARGPS is ARGPS = $\sum$ (regression coefficient of gene$_n$ × expression level of gene$_n$).

Development and validation of the ARGPS model

Using the median ARGPS as the cut-off value, we divided 335 GC patients into high-and low-risk groups and plotted Kaplan-Meier (KM) survival curves to probe into the significant differences in the overall survival (OS) between the two groups. The prognostic value of the ARGPS model was assessed through receiver operating characteristic (ROC) curves. By computing the area under the ROC curve (AUC) in a given year in R software, we can estimate the efficiency and accuracy of the model. As for three GEO datasets (GSE84437, GSE15459, GSE62254), the validating sets, the same processes were applied to test the predictive performance of the ARGPS system. Moreover, we adopted univariable and multivariable Cox regression analyses to evaluate the independent prognosis-related significance of this model. A nomogram was made to probably calculate the survival probability for GC patients. The C-index, calibration curve, and decision curve analysis (DCA) were served to estimate the performance and credibility of the nomogram (Vickers and Elkin, 2006; Fitzgerald et al., 2015; Kerr et al., 2016; Vickers et al., 2016).

Immune cell infiltration analysis

The CIBERSORT, a computational method, and Single-sample GSEA (ssGSEA), an extension of Gene Set Enrichment Analysis (GSEA), were applied synergistically to contrast the tumor immune microenvironment between the two groups (Newman et al., 2015). A leukocyte gene signature matrix file gained from CIBERSORTx website (https://cibersortx.stanford.edu/), was engaged to clarify the genetic signatures of 22 traditional immune cells. The four R packages ("GSVA", "GSEABase", "limma" and "Hmisc") and two websites [TIMER (https://cistrome.shinyapps.io/timer/) and TIMER 2.0 (http://timer.cistrome.org/)] were exploited to measure the correlation between markers, markers and immune cells (Ritchie et al., 2015; Li et al., 2016; Li et al., 2017; Li et al., 2020).

Mutation analysis

The somatic mutation of GC patients in the TCGA cohort was also obtained from the TCGA database (https://portal.gdc.cancer.gov/). The differences in somatic mutation data between the two risk groups were examined and took the form of waterfall graphs. The "maftool" R package was applied to calculate tumor mutation burden (TMB), referring to the number of tumor mutations per megabase in each tumor sample.

Statistical analysis

R software version 4.2.0 served as the tool for statistical analyses. p-value <0.05 was viewed as statistically significant.

Results

Identification of anoikis-related prognostic genes

Figure 1 displayed the flow diagram of this study. 15,121 genes were retained through batch effect removal. 1482 DEGs were filtered in the variance analysis between cancerous and adjacent normal samples in the TCGA dataset (|logFC| > 1.0, p.adj< 0.05) (Supplementary Table S2; Figure 2A). Then, we got 141 anoikis-related DEGs by intersecting DEGs with ARGs, which was displayed by the Venn diagram (Figure 2B). GO and KEGG functional enrichment analysis on these genes were carried out to scrutinize the function of the ARGs on GC development. The result of GO analysis revealed that they were enriched in the intrinsic, extrinsic, and regulated apoptotic signaling pathways in the biological process part, and collagen-containing extracellular matrix, an indispensable substance for anoikis, in the cell component part, signifying that anoikis played a huge part in the development of GC (Figure 2C). In the KEGG analysis, the most plenteous pathways were "Human papillomavirus infection", "MicroRNAs in cancer" and "Human T-cell leukemia virus one infection" (Figure 2D). By performing a univariable Cox regression analysis on GC patients of TCGA-STAD and GSE84437 cohorts, we gained 20 and 43 ARGs significantly associated with GC prognosis, separately. The forest plots described the detail (Figures 3A,B).

Development and validation of the ARGPS model

We intersected the results of two univariable Cox regression analyses and got 10 potential ARGs markers (PDK4, SKP2, EZH2, NOX4, PDGFRB, MMP11, SERPINE1, DNMT1, THY1, SNCG). Taking the TCGA cohort as the training set, lasso Cox regression was carried out on the ten candidate genes to identify the prognostic markers (Figures 3C,D). According to the regression analysis result, an ARGPS model was established as follows: ARGPS = 0.116 × PDK4 exp + (−0.340) × EZH2 exp +0.297 × NOX4 exp +0.108 × MMP11 exp +0.247 × SERPINE1 exp

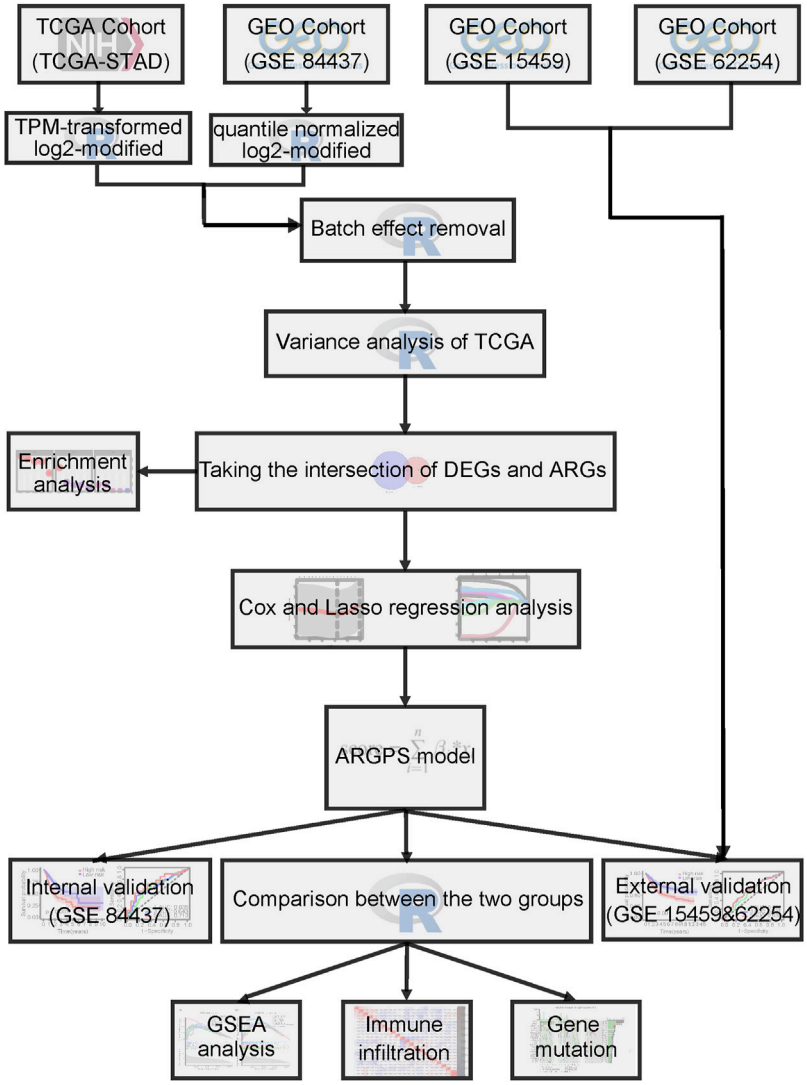

FIGURE 1
Drawing of the flow chart in this study.

+ (−0.412) × DNMT1 exp +0.243 × SNCG exp. Based on the median ARGPS, GC patients of the TCGA cohort were classified into the high- and low-risk groups. The risk score distribution and scatter plots were mapped to indicate that GC patients with a high-risk score, had shorter survival times and a higher proportion of death (Figure 4A). Then, the KM curve illustrated that the OS of patients in the high-risk group was lower, meaning a poorer prognosis (Figure 4B). Next, we calculated the three- and five-year AUC values under the time-dependent ROC curves were 0.643 and 0.713, respectively, suggesting specificity and sensitivity of the ARGPS in prognostic prediction (Figure 4C). Furthermore, to evaluate whether the ARGPS model is suitable for other datasets, we selected GSE84437 and two additional independent GEO datasets (GSE15459, GSE62254) as validation cohorts, grouped GC patients, and did the same analyses. The same results as the training set (TCGA) were also observed, proving the excellent stability and predictive efficacy of the ARGPS (Figures 4D–L). The clinical characteristics of GC patients in four cohorts were shown in Table 1.

Validation of a nomogram

A heat map illustrated the differences in the seven model genes expression and the distribution of clinicopathological features between two risk groups in the training set

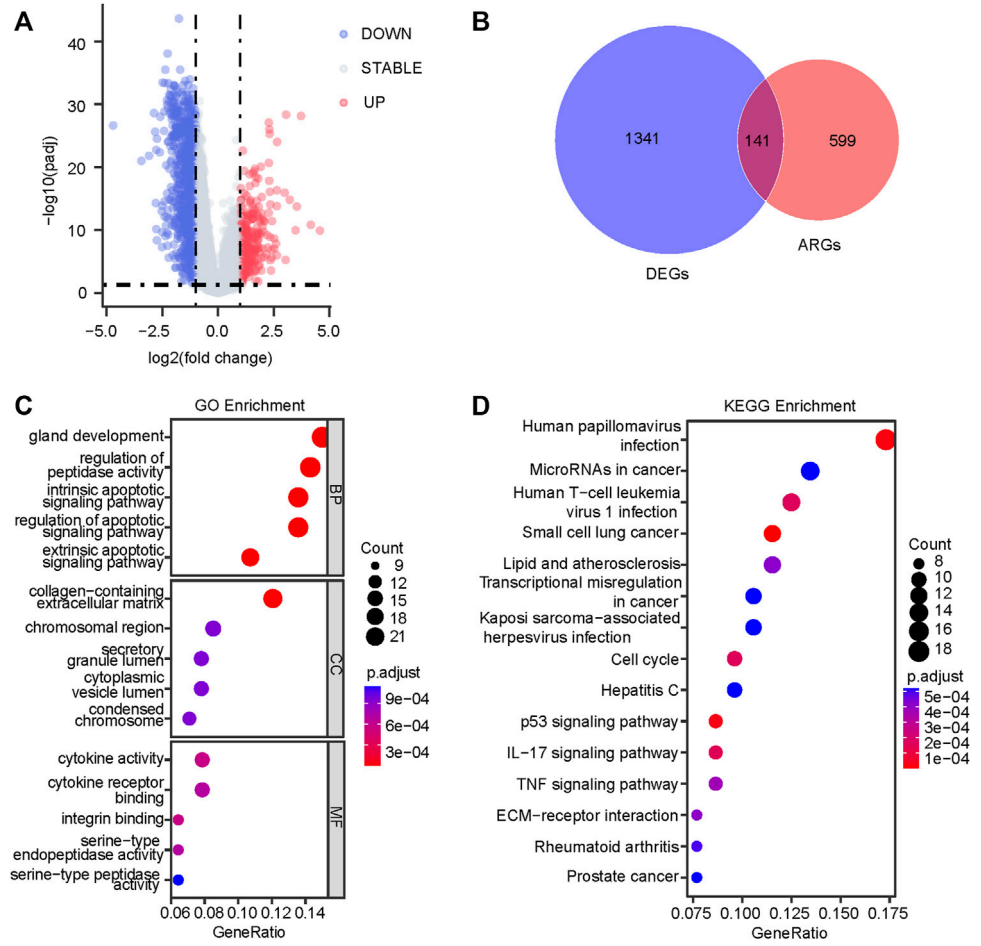

FIGURE 2
Identification of the anoikis-related prognostic genes. **(A)** The variance analysis between tumor and adjacent normal tissues in the TCGA dataset (|logFC| > 1.0, p.adj< 0.05). **(B)** The insection between 1482 DEGs and 740 ARGs is displayed by the Venn diagram. The dot plots of GO **(C)** and KEGG **(D)** enrichment analysis are based on 141 anoikis-related DEGs. TCGA, The Cancer Genome Atlas; DEGs, differentially expressed genes; ARGs, anoikis-related genes; GO, Gene Ontology; KEGG, Kyoto Encyclopedia of Genes and Genomes.

(Figure 5A). In combination with the clinical features of GC patients, we performed the univariable and multivariable Cox regression analyses and the result showed the independent prognostic predictability of the ARGPS (Figures 5B–D). Given the inconvenient clinical utility of the ARGPS, a hybrid nomogram model was created for predicting the survival probability of GC patients in a given year (Figure 5E). The result showed that C-index was 0.687, denoting the great reliability of the nomogram. Calibration curves of the OS at 1, 3, and 5 years were evenly distributed diagonally, proving the pretty fitness of the model (Figure 5F). Additionally, from DCA curves and AUC values, in clinical decision-making, the ARGPS model was found to be able to serve as the most effective prognostic indicator among other clinical characteristics (Figures 5D,G).

ARGPS model and functional analysis, gene mutation

For the purpose of further elucidating the underlying mechanisms of the impact of ARGPS on prognosis, KEGG and HALLMARK gene sets were selected to search for significantly enriched pathways between the two risk groups. In the high-risk group, the genes were mostly enriched in antigen processing and presentation, extracellular matrix (ECM) receptor interaction, protein export, proteasome, and ribosome in the KEGG part, and angiogenesis, mitotic spindle, protein secretion, reactive oxygen species pathway, and TGF-beta signaling in the HALLMARK part (Figures 6A,B). Detailed enrichment pathways and parameters are shown in Supplementary Tables S3, S4. Waterfall plots were exploited to analyze the somatic mutations in the two risk groups. From

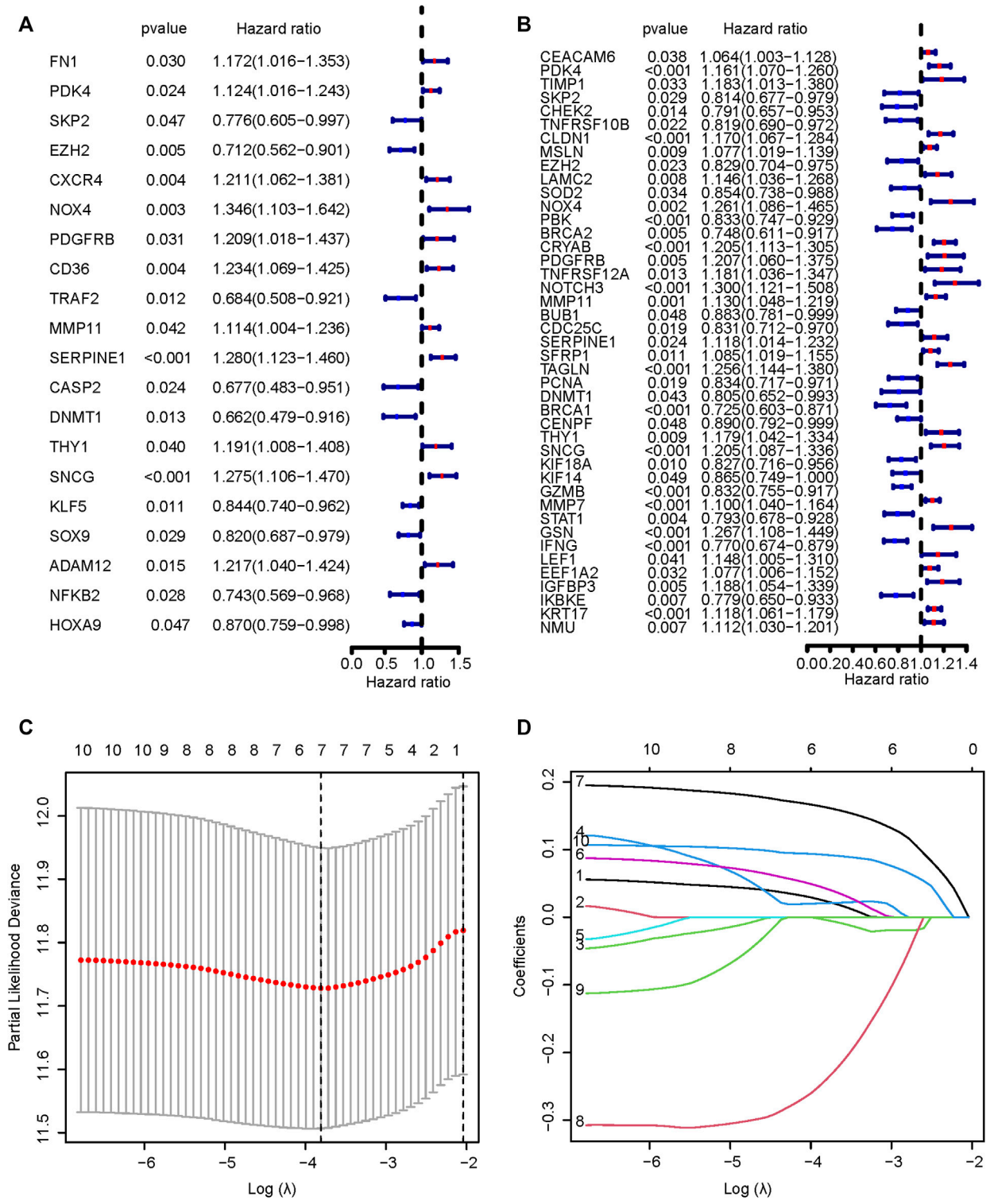

FIGURE 3
Univariable Cox regression analysis. The results of univariable Cox regression analyses of TCGA **(A)** and GEO **(B)** cohorts. **(C,D)** The results of LASSO analysis of ten prognostic ARGs. TCGA, The Cancer Genome Atlas; GEO, Gene Expression Omnibus; LASSO, Least Absolute Shrinkage and Selection Operator; ARGs, anoikis-related genes.

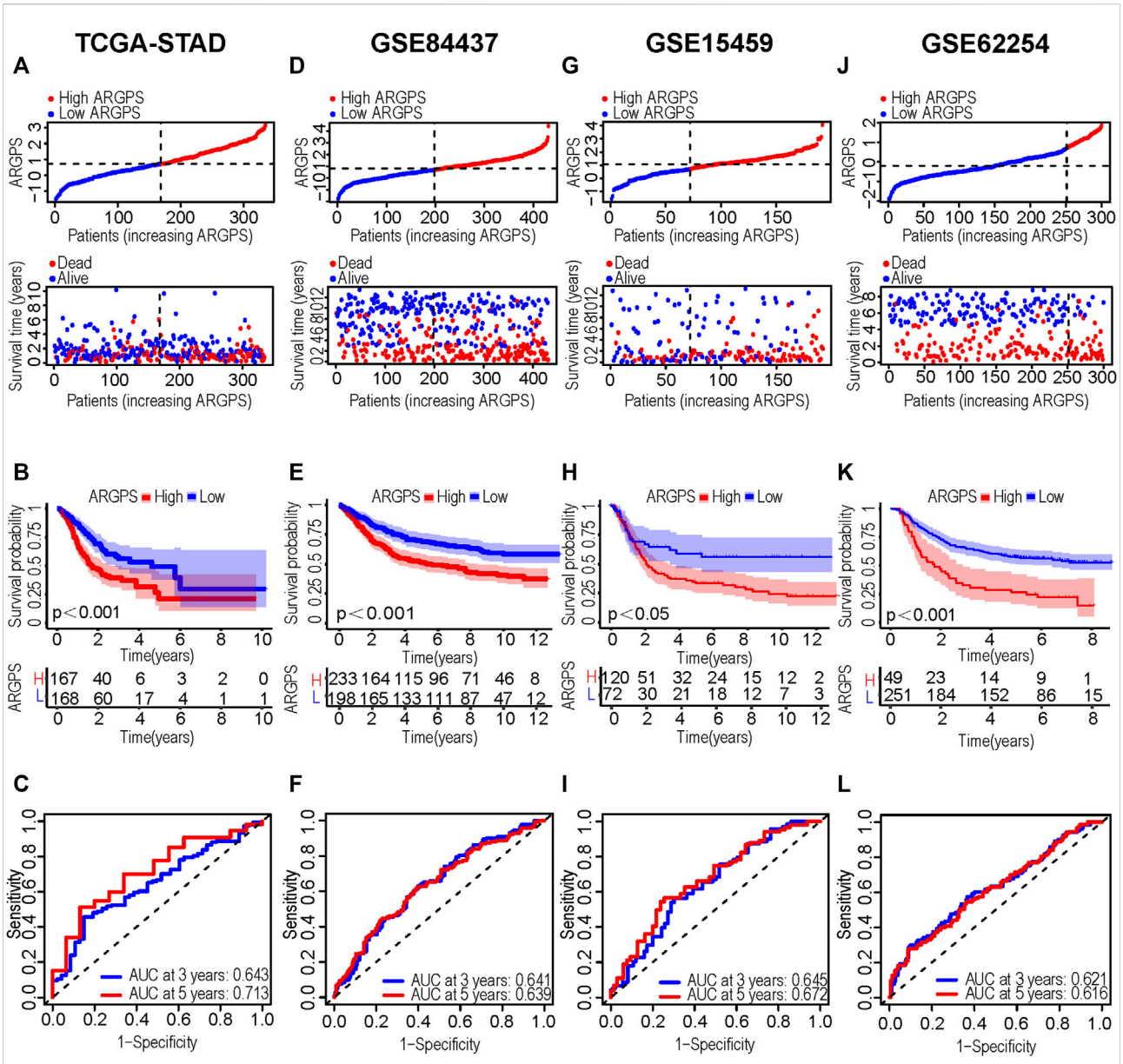

FIGURE 4
Construction and validation of the ARGPS model. **(A,D, G,J)** Distribution of ARGPS and relationship between ARGPS and survival status in the training and three testing sets. **(B,E,H,K)** The K-M survival curves of the high- and low-ARGPS groups in the training and three testing sets. **(C,F,I,L)** The time-dependent ROC curves for predicting OS at 3 and 5 years in the training and three testing sets. ARGPS, anoikis-related gene prognostic score; KM, Kaplan-Meier; ROC, receiver operating characteristic; OS, overall survival.

Figures 6C,D, the most common type of mutations in both groups was missense mutations, followed by Multi_Hit, which means that a gene has multiple mutations in the same sample. In the high-risk group, the overall levels of TMB were lower than those in the other group, which is contrary to our conventional understanding. Besides that, all mutant genes shown in the graphs were mutated less frequently in the high-risk group.

ARGPS model and immune infiltration

To explore whether and how the ARGPS model influenced the tumor immune landscape, bar graphs were first drawn to show the relative proportion of 22 different immune cells in every sample of the TCGA cohort (Figure 7A). The ssGSEA analysis was applied to study deeply the discrepancy between the immune status of the two risk groups. For type analysis of

10.3389/fgene.2022.1087201

TABLE 1 Clinical characteristics of GC patients in TCGA and three GEO cohorts.

Characteristics	TCGA-STAD (*n* = 335)	GSE84437 (*n* = 433)	GSE15459 (*n* = 192)	GSE62254 (*n* = 300)
	No. of patients (%)	No. of patients (%)	No. of patients (%)	No. of patients (%)
Age				
≤65	153 (45.67)	283 (65.36)	101 (52.60)	172 (57.33)
>65	179 (53.43)	150 (34.64)	91 (47.40)	128 (42.67)
unknown	3 (00.90)	0 (0.00)	0 (0.00)	0 (0.00)
Gender				
Male	217 (64.78)	296 (68.36)	125 (65.10)	199 (66.33)
Female	118 (35.22)	137 (31.64)	67 (34.90)	101 (33.67)
Grade				
G1	9 (2.69)	NA	NA	NA
G2	120 (35.82)	NA	NA	NA
G3	197 (58.80)	NA	NA	NA
Unknown	9 (2.69)	NA	NA	NA
Stage				
Stage I	44 (13.13)	NA	31 (16.15)	30 (10.00)
Stage II	107 (31.94)	NA	29 (15.10)	96 (32.00)
Stage III	137 (40.90)	NA	72 (37.50)	95 (31.67)
Stage IV	33 (9.85)	NA	60 (31.25)	77 (25.66)
Unknown	14 (4.18)	NA	0 (0.00)	2 (0.67)
T				
T1	15 (4.48)	11 (2.54)	NA	0 (0.00)
T2	73 (21.79)	38 (8.78)	NA	186 (62.00)
T3	155 (46.27)	92 (21.24)	NA	91 (30.33)
T4	88 (26.27)	292 (67.44)	NA	21 (7.00)
Unknown	4 (1.19)	0 (0.00)	NA	2 (0.67)
N				
N0	98 (29.25)	80 (18.48)	NA	38 (12.67)
N1	91 (27.17)	188 (43.42)	NA	131 (43.67)
N2	67 (20.00)	132 (30.49)	NA	80 (26.66)
N3	68 (20.30)	33 (7.62)	NA	51 (12.00)
Unknown	11 (3.28)	0 (0.00)	NA	0 (0.00)
M				
M0	302 (90.15)	NA	NA	273 (91.00)
M1	21 (6.27)	NA	NA	27 (9.00)
Unknown	12 (3.58)	NA	NA	0 (0.00)

TCGA, The Cancer Genome Atlas; GEO, Gene Expression Omnibus.

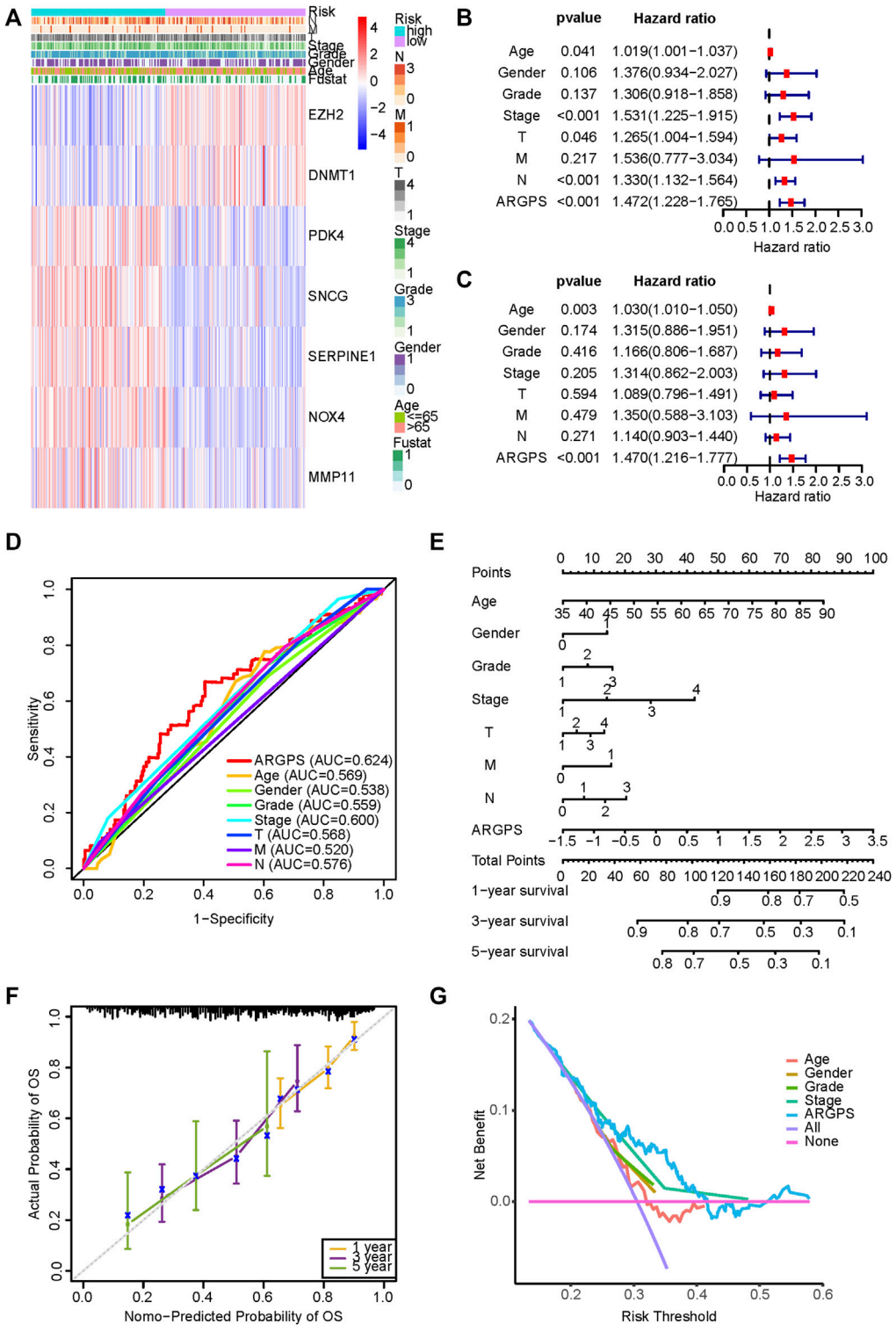

FIGURE 5
Validation of ARGPS's ability to predict the prognosis of gastric cancer. **(A)** The differences in the expression of seven markers and the distribution of clinicopathological features between the two risk groups in the TCGA cohort were plotted by the heat map. The results of univariable **(B)** and multivariable Cox regression analysis **(C)** between ARGPS and clinicopathological factors. **(D)** The ROC curves based on the ARGPS model and other clinicopathological factors in the TCGA cohort. **(E)** Nomogram based on ARGPS and clinicopathological features in the TCGA cohort. **(F)** Calibration curves for the validation of the nomogram. **(G)** DCA curves of the clinical utility between ARGPS and other clinical factors regarding the overall survival (OS) in the TCGA cohort. TCGA, The Cancer Genome Atlas; ARGPS, anoikis-related gene prognostic score; ROC, receiver operating characteristic; DCA, Decision curve analysis.

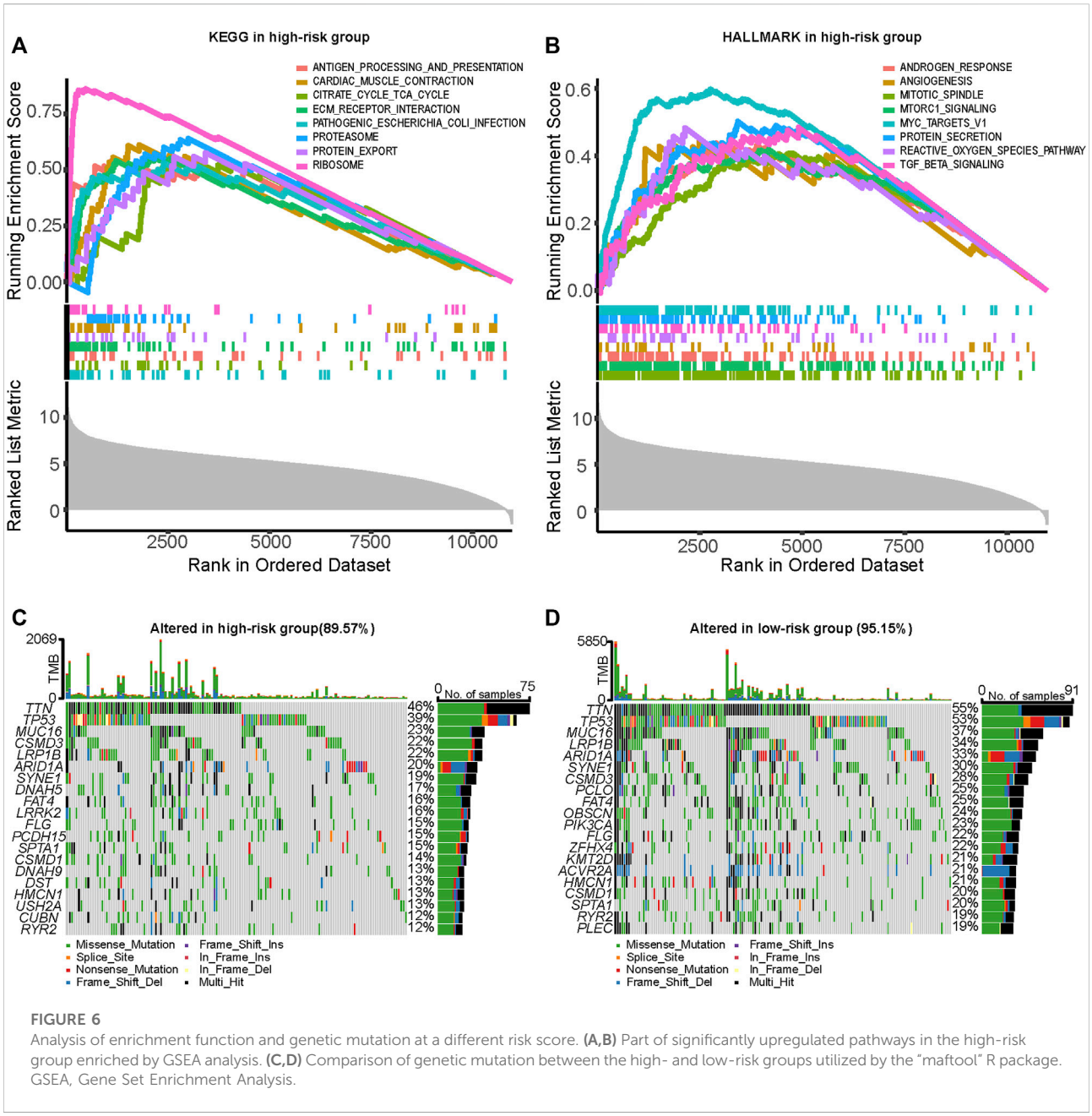

FIGURE 6
Analysis of enrichment function and genetic mutation at a different risk score. **(A,B)** Part of significantly upregulated pathways in the high-risk group enriched by GSEA analysis. **(C,D)** Comparison of genetic mutation between the high- and low-risk groups utilized by the "maftool" R package. GSEA, Gene Set Enrichment Analysis.

28 immune cells, we discovered that compared to GC patients with a lower risk score, those with a higher risk score had significantly higher infiltration of multiple cells (including activated B cell, central and effector memory T cell, immature B cell, regulatory T cell, T follicular helper cell, type 1 T helper cell, activated dendritic cell, CD56 bright natural killer cell, eosinophil, immature dendritic cell, macrophage, mast cell, MDSC, natural killer cell, natural killer T cell, and plasmacytoid dendritic cell), whereas lower infiltration of activated CD4 T cell (Figure 7B). For type analysis of 13 immune pathways, multiple pathways (including APC co-stimulation, CCR, check-point, HLA, parainflammation, type I and II interferon response) of the high-risk group were also significantly more vibrant than those of the low-risk group, which may work for the worse prognosis of the GC patients (Figure 7C). Furthermore, the heat maps were painted to show the strong relationship of the seven markers to immune cells and pathways (Figures 8A,B). In addition, the TIMER database was available to predict the relation between the markers. Figure 8C plotted the linear correlation of each of the two markers, indicating the intense relationship between the seven markers.

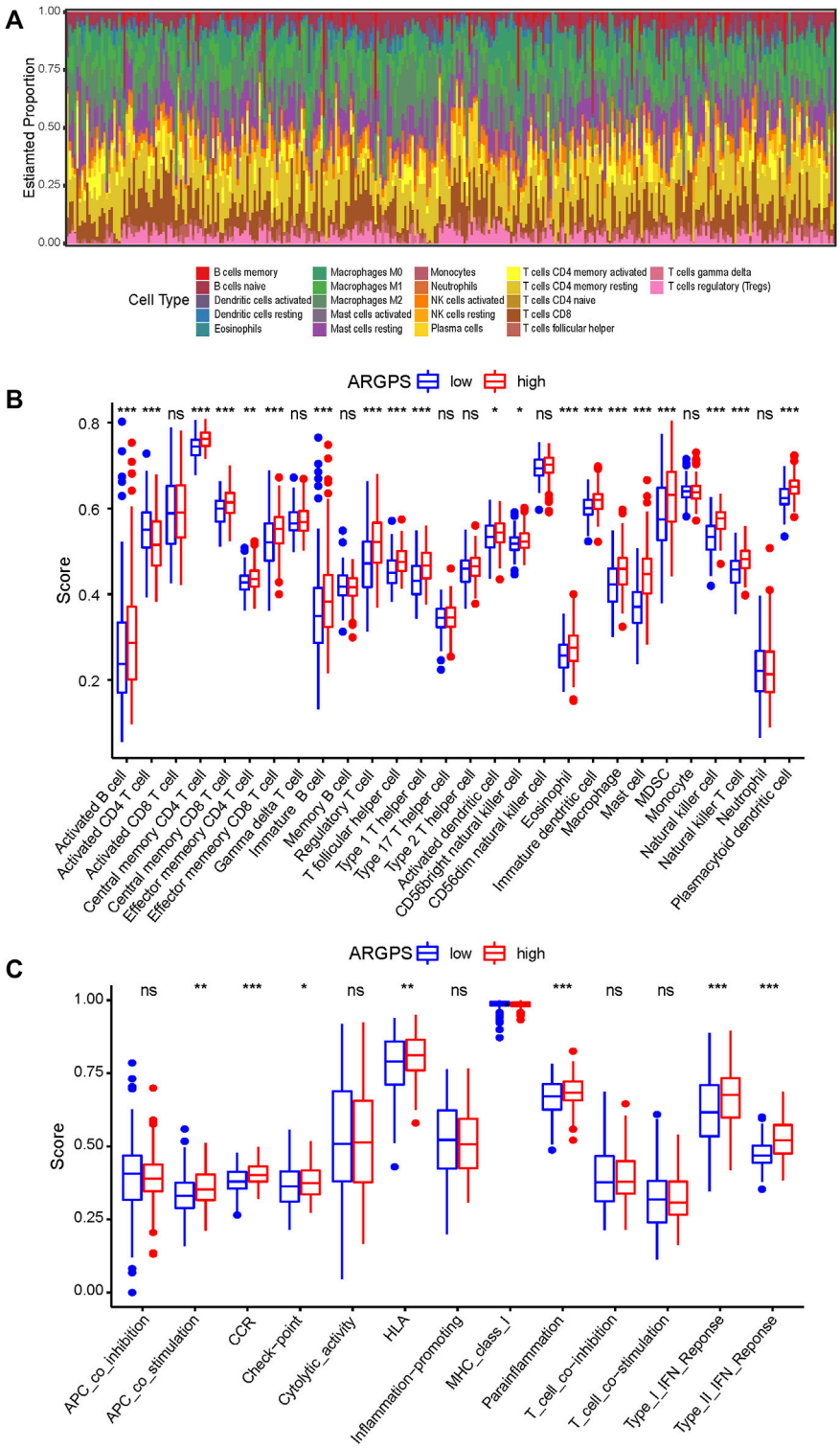

FIGURE 7
Evaluation of the immune microenvironment of gastric cancer. **(A)** The proportion and distribution of 22 immune cells in each sample of the TCGA cohort were calculated by the CIBERSORT algorithm. The sum of all estimated cell scores in each sample is 1. The difference of **(B)** 28 immune cells and **(C)** 13 immune pathways infiltration levels between the high- and low-risk groups compared by the ssGSEA analysis. ns > 0.05, *<0.05, **<0.01, ***<0.001. TCGA, The Cancer Genome Atlas; ssGSEA, Single-sample Gene Set Enrichment Analysis.

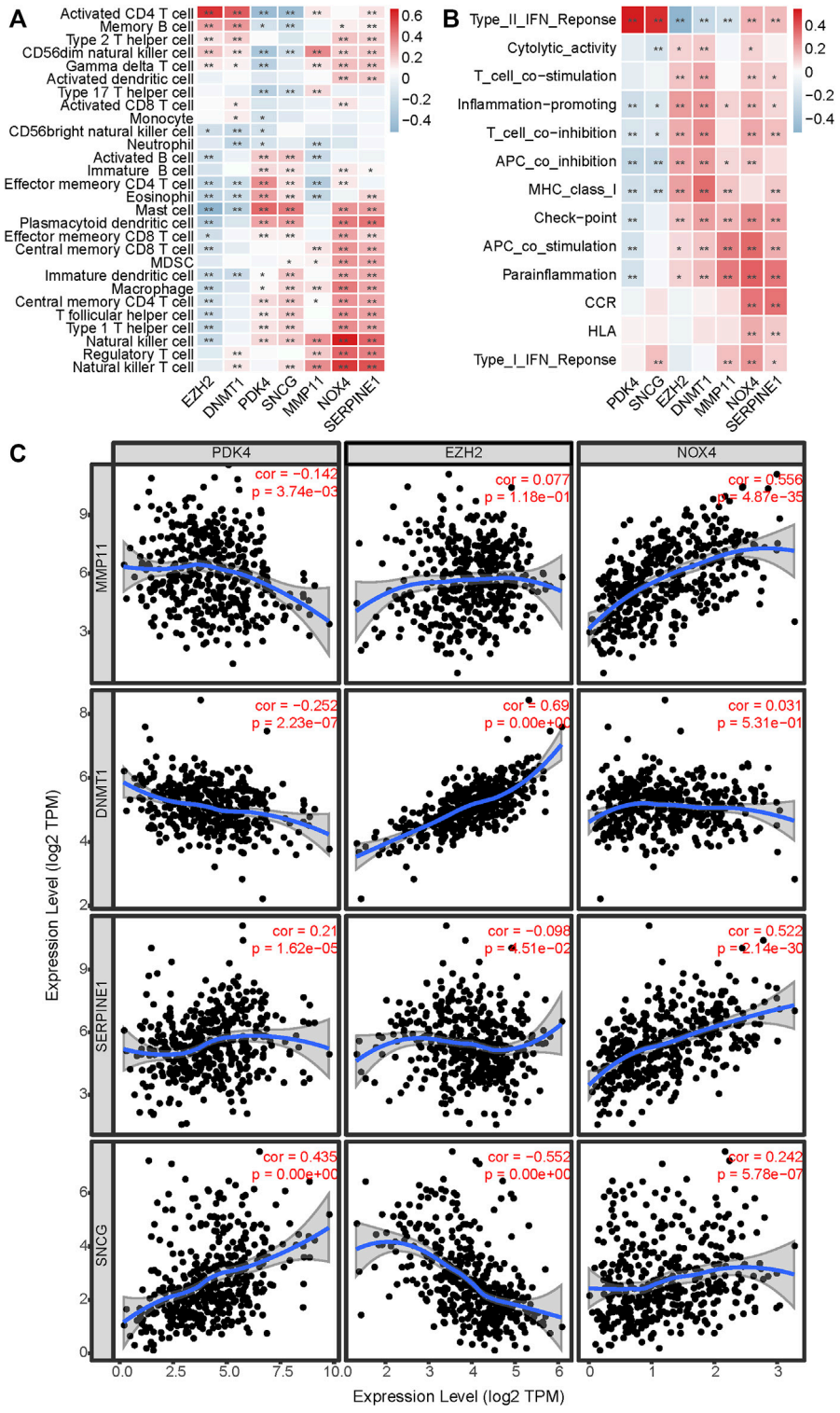

FIGURE 8
Estimation of the correlation between markers and immune infiltration. The correlation between the seven markers and **(A)** 28 immune cells and **(B)** 13 immune pathways showed by heat maps. **(C)** The linear relation of each of the two markers in the model is predicted by TIMER. *< 0.05, **< 0.01.

Discussion

Previously, there were some reports in the literature about the effects of anoikis on GC. Kai Wang et al. sequenced the whole genomes of gastric cancer tissues and performed comprehensive molecular profiling, discovering that RHOA hotspot mutants could facilitate anoikis escape in the organoid cultures (Wang et al., 2014a). Numbers of molecules and pathways have been confirmed to be involved in the anoikis resistance, which resulted in the metastasis and progression of GC (Li et al., 2020b; Ye et al., 2020; Zhang et al., 2022a; Li et al., 2022b). In addition, by reducing anoikis resistance and cancer cell mobility, some drugs could trigger apoptosis and inhibit metastasis, thereby delaying the progression of GC (Kim et al., 2022). All of the above emphasized that the notion of targeting genes associated with anoikis might be imperative to control tumor development and progression. As we know, in GC, this study is the first to identify anoikis-related prognostic biomarkers and construct a relevant predictive model to evaluate patient outcomes.

In this research, we screened out seven genes related to the prognosis of GC, which contained PDK4, EZH2, NOX4, MMP11, SERPINE1, DNMT1, and SNCG, and created a predictive risk score model, namely ARGPS model. Certain interactions between these markers and tumor initiation and progression have been described in studies before. For example, Zimu Zhang et al. disclosed that PDK4 promoted invasion and migration ability of GC cells (Zhang et al., 2022b). In the high-PDK4 group, enriched functional pathways were correlated with cell adhesion regulation and synaptic activity, which were substantial in cancer anoikis resistance, proliferation, invasion, and metastasis (Zhong and Rescorla, 2012; Alanko et al., 2015; Zhang et al., 2022b). *In vitro* studies demonstrated that EZH2 bound to the vital tumor suppressor PTEN locus and led to proliferation, invasion, and pluripotent phenotype of GC cells (Gan et al., 2018). IL-6/STAT3 signaling, whose aberrant expression in GC cells was thought to be a main mechanism for tumorigenesis and pathogenesis, drove EZH2 transcriptional stimulation and mediated unfortunate outcome (Yu and Jove, 2004; Yu et al., 2009; Li et al., 2010; Pan et al., 2016). NOX4, one of the major origins of reactive oxygen species (ROS), played a crucial role in genomic instability, resistance to anoikis, migration, and extravasation into distant sites (Bedard and Krause, 2007; Liou and Storz, 2010; Peiris-Pages et al., 2015; Schumacker, 2015). The expression of NOX4 in GC was significantly relevant to tumor size, lymph node metastasis, venous invasion, and unfortunate survival (Du et al., 2019). What is interesting is that NOX4 could enhance cell propagation by activating the GLI1 transcription factor, which was a distinguished molecule in the Hedgehog signaling pathway (Briscoe and Therond, 2013; Tang et al., 2018). Meanwhile, it was verified that the suppression of GLI1 protein could evoke anoikis *in vitro* and prevent tumor formation *in vivo* (Kandala and Srivastava, 2012). Similarly, SERPINE1, a key inhibitor of tissue plasminogen activator and urokinase, is abundant in tumor tissues and strongly interrelated with the propagation and invasiveness of GC cells (Chen et al., 2022). SERPINE1 could induce angiogenesis and tumor inflammatory microenvironment, in which anoikis was a critical player, by regulating the expression level of VEGF and IL-6 *via* VEGF and JAK-STAT3 inflammatory pathways (Sakamoto and Kyprianou, 2010; Feng et al., 2014; Teng et al., 2021; Chen et al., 2022). Y-B Kou et al. discovered that the growth, expansion, and invasion activities of GC cells could be inhibited by the knockdown of MMP11, probably through downregulation of the PCNA, IGF-1, and VEGF (Kou et al., 2013). In addition, MMP11 in exosomes secreted from gastric cancer-associated fibroblasts can be delivered into GC cells to partially accelerate their progression and metastasis (Xu et al., 2019). DNMT1, whose full name is DNA methyltransferase 1, is one of the DNA-modifying enzymes (Lyko, 2018). It might participate in the modulation of DNA methylation levels and give rise to the development of an anoikis-resistance phenotype (Campos et al., 2007; Lyko, 2018). Recently, a study suggested that lncRNA SAMD12-AS1 potentially played oncogenic roles in GC by directly bounding to DNMT1 and enabling DNMT1 to restrain the P53 signal pathway (Lu et al., 2021a). A strong interaction between the expression level of SNCG, a pro-metastatic oncogene, in primary and metastatic sites has been revealed in many solid tumor types (Liu et al., 2005). In addition, SNCG expression in GC tissues, particularly in metastatic tissues, was relevant to tumor microenvironment and metastasis (Hu et al., 2009; Wang et al., 2014b). Thus, hypoxia-inducible lncRNA-AK058003 could increase GC metastasis by targeting SNCG (Wang et al., 2014b). It is worth noting that markers did not work alone but had some linkages. For instance, the synergistic mediation of methylation by EZH2 and DNMT1 contributed to the progression of GC (Ning et al., 2015).

Based on ARGPS we calculated, GC patients were separated into high- and low-risk groups. Follow-up analyses revealed that the GC patients with the high-risk score correlated with a poorer prognosis, which was confirmed by three testing cohorts (GSE84437, GSE15459, GSE62254). The results of univariable and multivariable Cox analyses with other clinical confounding factors showed extraordinary standalone prediction value of ARGPS. Then, a nomogram was built to accurately quantify personalized predictive scores and survival probabilities. Both C-index and the calibration curves showed superb consistency. Additionally, decision curve analysis was used to suggest the potential clinical utility of the model.

We compared the differences in functional pathways and somatic mutations between the two groups. GSEA analyses have enriched ECM receptor interaction and reactive oxygen species pathways, which were highly related to anoikis (Tang et al., 2018). Moreover, these results suggested that anoikis might closely connect with immune invasion, material transportation, and angiogenesis in GC. Intriguingly, not only

the overall pattern of gene mutations was lower in the high score group but also the mutation frequency of commonly mutated genes was lower. The difference in TMB between the two groups was confirmed to be statistically significant by the Wilcoxon rank sum test. Although most genetic mutations (such as missense mutations) were harmful or lethal to the body, the possibility of beneficial effects could not be entirely ruled out. A panel-based sequencing study of advanced gastric cancer showed that patients with elevated TMB had higher objective response rates and longer progression-free survival, suggesting that TMB could be employed as a potential predictive biomarker (Kim et al., 2020). Among patients with advanced gastric cancer who received neoadjuvant chemotherapy before radical gastrectomy, those with high TMB showed favorable treatment response and better disease-free survival (Li et al., 2021). Besides, in multiple cancer types, TMB was considered as another indicator of patients' response to immunotherapy because a positive correlation between TMB and benefit of immunotherapy was observed in a comprehensive analysis (Hodges et al., 2017; Yarchoan et al., 2017).

Epigenomic alterations in cancer interact with the immune microenvironment to dictate tumor evolution and therapeutic response (Sundar et al., 2022). Though a variety of programmed cell death modes (e.g., necroptosis, pyroptosis, ferroptosis, *etc.*) have been showed to be associated with tumor immunity, the correlation between anoikis and immunity is still unclear (Gao et al., 2022; Niu et al., 2022). We managed to explore the differences in the immune landscape between the two groups, showing that in the high score group with the worrisome outcomes, the proportion of most immune cells and functions were significantly increased, representing that anoikis may regulate tumor progression by affecting immune infiltration levels. If we think about this among all the different immune cells, there are both protumorigenic and antitumorigenic cells. One should note that one of the most crucial elements of the tumor immunosuppressive microenvironment are myeloid-derived suppressor cells (MDSCs), which plays an important role in *Helicobacter* pylori-induced intestinal metaplasia and tumor progression (Ding et al., 2016; Ding et al., 2020; Ding et al., 2022). Based on our results, MDSCs infiltration level was relatively high in the high-ARGPS group and was significantly related to SNCG, MMP11, NOX4 and SERPINE1. Besides, EZH2 and DNMT1 could regulate the differentiation and accumulation of MDSCs (Huang et al., 2019; Smith et al., 2020; Lu et al., 2021b; Yang et al., 2022). Due to the certainty of immunity on tumor progression and the uncertainty of anoikis on the immune landscape, the interaction between anoikis and immunity (especially MDSCs) might be an interesting field to research.

Though this study has made a breakthrough, it still is limited by some aspects. First, this study was confined to mining and analyzing public databases. Second, although the established model and nomogram had a pretty good predictive capability, taking the heterogeneity of the cells in tumor tissues into consideration, studies on anoikis executed at the single-cell level may shed light on the critical role of anoikis on the outcome of GC patients more accurately. Third, despite this study showing that there was a powerful relationship between the ARGs and immunity, the detailed mechanism was still not fully explained. Finally, the study has a lack of validation *in vivo* or *in vitro*. Through combined the results of this study with previous literature, we reasonably believe that the underlying mechanism of anoikis-related markers and gastric cancer immune microenvironment (especially MDSCs) seems to be full of promises and worthful for future investigation.

Conclusion

To sum up, our seven-gene ARGPS model is capable of predicting the outcome of GC patients, and the nomogram can assist the clinician to develop personalized treatment plans for various patients. More research in the future into the molecular interaction between anoikis and tumor is required to provide the theoretical basis for clinical practice and a road map for precision medicine.

Data availability statement

Publicly available datasets were analyzed in this study. This data can be found here: TCGA: https://portal.gdc.cancer.gov/ GEO: https://www.ncbi.nlm.nih.gov/geo/.

Author contributions

ZZ: conceptualization, methodology, software, data curation, and original draft writing. CL, YP, RL, and QL: data review. QL makes a great contribution to data analysis, manuscript review, and study supervision.

Funding

The study was funded by the National Natural Science Foundation of China (No. 81974064).

Acknowledgments

We are grateful for the public databases and various analytical methods used in this article.

Conflict of interest

The authors declare that the research was conducted in the absence of any commercial or financial relationships that could be construed as a potential conflict of interest.

Publisher's note

All claims expressed in this article are solely those of the authors and do not necessarily represent those of their affiliated organizations, or those of the publisher, the editors and the reviewers. Any product that may be evaluated in this article, or claim that may be made by its manufacturer, is not guaranteed or endorsed by the publisher.

Supplementary material

The Supplementary Material for this article can be found online at: https://www.frontiersin.org/articles/10.3389/fgene.2022.1087201/full#supplementary-material

References

Adeshakin, F. O., Adeshakin, A. O., Afolabi, L. O., Yan, D., Zhang, G., and Wan, X. (2021). Mechanisms for modulating anoikis resistance in cancer and the relevance of metabolic reprogramming. *Front. Oncol.* 11, 626577. doi:10.3389/fonc.2021.626577

Alanko, J., Mai, A., Jacquemet, G., Schauer, K., Kaukonen, R., Saari, M., et al. (2015). Integrin endosomal signalling suppresses anoikis. *Nat. Cell Biol.* 17 (11), 1412–1421. doi:10.1038/ncb3250

Bedard, K., and Krause, K. H. (2007). The NOX family of ROS-generating NADPH oxidases: Physiology and pathophysiology. *Physiol. Rev.* 87 (1), 245–313. doi:10.1152/physrev.00044.2005

Briscoe, J., and Therond, P. P. (2013). The mechanisms of Hedgehog signalling and its roles in development and disease. *Nat. Rev. Mol. Cell Biol.* 14 (7), 416–429. doi:10.1038/nrm3598

Campos, A. C., Molognoni, F., Melo, F. H. M., Galdieri, L. C., Carneiro, C. R. W., D'Almeida, V., et al. (2007). Oxidative stress modulates DNA methylation during melanocyte anchorage blockade associated with malignant transformation. *Neoplasia* 9 (12), 1111–1121. doi:10.1593/neo.07712

Chen, S., Li, Y., Zhu, Y., Fei, J., Song, L., Sun, G., et al. (2022). SERPINE1 overexpression promotes malignant progression and poor prognosis of gastric cancer. *J. Oncol.* 2022, 2647825. doi:10.1155/2022/2647825

Ding, L., Chakrabarti, J., Sheriff, S., Li, Q., Thi Hong, H. N., Sontz, R. A., et al. (2022). Toll-like receptor 9 pathway mediates schlafen(+)-MDSC polarization during helicobacter-induced gastric metaplasias. *Gastroenterology* 163 (2), 411–425 e4. doi:10.1053/j.gastro.2022.04.031

Ding, L., Hayes, M. M., Photenhauer, A., Eaton, K. A., Li, Q., Ocadiz-Ruiz, R., et al. (2016). Schlafen 4-expressing myeloid-derived suppressor cells are induced during murine gastric metaplasia. *J. Clin. Invest.* 126 (8), 2867–2880. doi:10.1172/JCI82529

Ding, L., Li, Q., Chakrabarti, J., Munoz, A., Faure-Kumar, E., Ocadiz-Ruiz, R., et al. (2020). MiR130b from Schlafen4(+) MDSCs stimulates epithelial proliferation and correlates with preneoplastic changes prior to gastric cancer. *Gut* 69 (10), 1750–1761. doi:10.1136/gutjnl-2019-318817

Du, S., Miao, J., Lu, X., Shi, L., Sun, J., Xu, E., et al. (2019). NADPH oxidase 4 is correlated with gastric cancer progression and predicts a poor prognosis. *Am. J. Transl. Res.* 11 (6), 3518–3530.

Feng, M. X., Ma, M. Z., Fu, Y., Li, J., Wang, T., Xue, F., et al. (2014). Elevated autocrine EDIL3 protects hepatocellular carcinoma from anoikis through RGD-mediated integrin activation. *Mol. Cancer* 13, 226. doi:10.1186/1476-4598-13-226

Fitzgerald, M., Saville, B. R., and Lewis, R. J. (2015). Decision curve analysis. *JAMA* 313 (4), 409–410. doi:10.1001/jama.2015.37

Frisch, S. M., and Francis, H. (1994). Disruption of epithelial cell-matrix interactions induces apoptosis. *J. Cell Biol.* 124 (4), 619–626. doi:10.1083/jcb.124.4.619

Frisch, S. M., and Screaton, R. A. (2001). Anoikis mechanisms. *Curr. Opin. Cell Biol.* 13 (5), 555–562. doi:10.1016/s0955-0674(00)00251-9

Gan, L., Xu, M., Hua, R., Tan, C., Zhang, J., Gong, Y., et al. (2018). The polycomb group protein EZH2 induces epithelial-mesenchymal transition and pluripotent phenotype of gastric cancer cells by binding to PTEN promoter. *J. Hematol. Oncol.* 11 (1), 9. doi:10.1186/s13045-017-0547-3

Gao, W., Wang, X., Zhou, Y., Wang, X., and Yu, Y. (2022). Autophagy, ferroptosis, pyroptosis, and necroptosis in tumor immunotherapy. *Signal Transduct. Target. Ther.* 7 (1), 196. doi:10.1038/s41392-022-01046-3

Guadamillas, M. C., Cerezo, A., and Del Pozo, M. A. (2011). Overcoming anoikis--pathways to anchorage-independent growth in cancer. *J. Cell Sci.* 124 (19), 3189–3197. doi:10.1242/jcs.072165

He, X., Wu, L., Dong, Z., Gong, D., Jiang, X., Zhang, H., et al. (2022). Real-time use of artificial intelligence for diagnosing early gastric cancer by magnifying image-enhanced endoscopy: A multicenter diagnostic study (with videos). *Gastrointest. Endosc.* 95 (4), 671–678 e4. doi:10.1016/j.gie.2021.11.040

Hodges, T. R., Ott, M., Xiu, J., Gatalica, Z., Swensen, J., Zhou, S., et al. (2017). Mutational burden, immune checkpoint expression, and mismatch repair in glioma: Implications for immune checkpoint immunotherapy. *Neuro. Oncol.* 19 (8), 1047–1057. doi:10.1093/neuonc/nox026

Hu, H., Sun, L., Guo, C., Liu, Q., Zhou, Z., Peng, L., et al. (2009). Tumor cell-microenvironment interaction models coupled with clinical validation reveal CCL2 and SNCG as two predictors of colorectal cancer hepatic metastasis. *Clin. Cancer Res.* 15 (17), 5485–5493. doi:10.1158/1078-0432.CCR-08-2491

Huang, S., Wang, Z., Zhou, J., Huang, J., Zhou, L., Luo, J., et al. (2019). EZH2 inhibitor GSK126 suppresses antitumor immunity by driving production of myeloid-derived suppressor cells. *Cancer Res.* 79 (8), 2009–2020. doi:10.1158/0008-5472.CAN-18-2395

Kandala, P. K., and Srivastava, S. K. (2012). Diindolylmethane-mediated Gli1 protein suppression induces anoikis in ovarian cancer cells *in vitro* and blocks tumor formation ability *in vivo*. *J. Biol. Chem.* 287 (34), 28745–28754. doi:10.1074/jbc.M112.351379

Kanehisa, M., Furumichi, M., Sato, Y., Ishiguro-Watanabe, M., and Tanabe, M. (2021). Kegg: Integrating viruses and cellular organisms. *Nucleic Acids Res.* 49 (D1), D545–D551. doi:10.1093/nar/gkaa970

Kanehisa, M., and Goto, S. (2000). Kegg: Kyoto Encyclopedia of genes and genomes. *Nucleic Acids Res.* 28 (1), 27–30. doi:10.1093/nar/28.1.27

Kerr, K. F., Brown, M. D., Zhu, K., and Janes, H. (2016). Assessing the clinical impact of risk prediction models with decision curves: Guidance for correct interpretation and appropriate use. *J. Clin. Oncol.* 34 (21), 2534–2540. doi:10.1200/JCO.2015.65.5654

Khan, S. U., Fatima, K., and Malik, F. (2022). Understanding the cell survival mechanism of anoikis-resistant cancer cells during different steps of metastasis. *Clin. Exp. Metastasis* 39 (5), 715–726. doi:10.1007/s10585-022-10172-9

Kim, J., Kim, B., Kang, S. Y., Heo, Y. J., Park, S. H., Kim, S. T., et al. (2020). Tumor mutational burden determined by panel sequencing predicts survival after immunotherapy in patients with advanced gastric cancer. *Front. Oncol.* 10, 314. doi:10.3389/fonc.2020.00314

Kim, M. J., Kawk, H. W., Kim, S. H., Lee, H. J., Seo, J. W., Lee, C. Y., et al. (2022). The p53-driven anticancer effect of ribes fasciculatum extract on AGS gastric cancer cells. *Life (Basel)* 12 (2), 303. doi:10.3390/life12020303

Kim, Y. N., Koo, K. H., Sung, J. Y., Yun, U. J., and Kim, H. (2012). Anoikis resistance: An essential prerequisite for tumor metastasis. *Int. J. Cell Biol.* 2012, 306879. doi:10.1155/2012/306879

Kou, Y. B., Zhang, S. Y., Zhao, B. L., Ding, R., Liu, H., and Li, S. (2013). Knockdown of MMP11 inhibits proliferation and invasion of gastric cancer cells. *Int. J. Immunopathol. Pharmacol.* 26 (2), 361–370. doi:10.1177/039463201302600209

Krejs, G. J. (2010). Gastric cancer: Epidemiology and risk factors. *Dig. Dis.* 28 (4-5), 600–603. doi:10.1159/000320277

Li, B., Severson, E., Pignon, J. C., Zhao, H., Li, T., Novak, J., et al. (2016). Comprehensive analyses of tumor immunity: Implications for cancer immunotherapy. *Genome Biol.* 17, 174. doi:10.1186/s13059-016-1028-7

Li, J., Zhu, Y., Dong, Z., He, X., Xu, M., Liu, J., et al. (2022). Development and validation of a feature extraction-based logical anthropomorphic diagnostic system for early gastric cancer: A case-control study. *EClinicalMedicine* 46, 101366. doi:10.1016/j.eclinm.2022.101366

Li, S., Wu, T., Lu, Y. X., Wang, J. X., Yu, F. H., Yang, M. Z., et al. (2020). Obesity promotes gastric cancer metastasis via diacylglycerol acyltransferase 2-dependent lipid droplets accumulation and redox homeostasis. *Redox Biol.* 36, 101596. doi:10.1016/j.redox.2020.101596

Li, T. W., Fan, J., Wang, B., Traugh, N., Chen, Q., Liu, J. S., et al. (2017). Timer: A web server for comprehensive analysis of tumor-infiltrating immune cells. *Cancer Res.* 77 (21), E108–E110. doi:10.1158/0008-5472.CAN-17-0307

Li, T. W., Fu, J., Zeng, Z., Cohen, D., Li, J., Chen, Q., et al. (2020). TIMER2.0 for analysis of tumor-infiltrating immune cells. *Nucleic Acids Res.* 48 (W1), W509–W514. doi:10.1093/nar/gkaa407

Li, Y., de Haar, C., Chen, M., Deuring, J., Gerrits, M. M., Smits, R., et al. (2010). Disease-related expression of the IL6/STAT3/SOCS3 signalling pathway in ulcerative colitis and ulcerative colitis-related carcinogenesis. *Gut* 59 (2), 227–235. doi:10.1136/gut.2009.184176

Li, Y., Liu, C., Zhang, X., Huang, X., Liang, S., Xing, F., et al. (2022). CCT5 induces epithelial-mesenchymal transition to promote gastric cancer lymph node metastasis by activating the Wnt/β-catenin signalling pathway. *Br. J. Cancer* 126 (12), 1684–1694. doi:10.1038/s41416-022-01747-0

Li, Z., Jia, Y., Zhu, H., Xing, X., Pang, F., Shan, F., et al. (2021). Tumor mutation burden is correlated with response and prognosis in microsatellite-stable (MSS) gastric cancer patients undergoing neoadjuvant chemotherapy. *Gastric Cancer* 24 (6), 1342–1354. doi:10.1007/s10120-021-01207-3

Liou, G. Y., and Storz, P. (2010). Reactive oxygen species in cancer. *Free Radic. Res.* 44 (5), 479–496. doi:10.3109/10715761003667554

Liu, H., Liu, W., Wu, Y., Zhou, Y., Xue, R., Luo, C., et al. (2005). Loss of epigenetic control of synuclein-gamma gene as a molecular indicator of metastasis in a wide range of human cancers. *Cancer Res.* 65 (17), 7635–7643. doi:10.1158/0008-5472.CAN-05-1089

Lu, G. H., Zhao, H. M., Liu, Z. Y., Cao, Q., Shao, R. D., and Sun, G. (2021). LncRNA SAMD12-AS1 promotes the progression of gastric cancer via DNMT1/p53 Axis. *Arch. Med. Res.* 52 (7), 683–691. doi:10.1016/j.arcmed.2021.04.004

Lu, W., Cao, F., Feng, L., Song, G., Chang, Y., Chu, Y., et al. (2021). LncRNA Snhg6 regulates the differentiation of MDSCs by regulating the ubiquitination of EZH2. *J. Hematol. Oncol.* 14 (1), 196. doi:10.1186/s13045-021-01212-0

Lyko, F. (2018). The DNA methyltransferase family: A versatile toolkit for epigenetic regulation. *Nat. Rev. Genet.* 19 (2), 81–92. doi:10.1038/nrg.2017.80

Newman, A. M., Liu, C. L., Green, M. R., Gentles, A. J., Feng, W., Xu, Y., et al. (2015). Robust enumeration of cell subsets from tissue expression profiles. *Nat. Methods* 12 (5), 453–457. doi:10.1038/nmeth.3337

Ning, X., Shi, Z., Liu, X., Zhang, A., Han, L., Jiang, K., et al. (2015). DNMT1 and EZH2 mediated methylation silences the microRNA-200b/a/429 gene and promotes tumor progression. *Cancer Lett.* 359 (2), 198–205. doi:10.1016/j.canlet.2015.01.005

Niu, X., Chen, L., Li, Y., Hu, Z., and He, F. (2022). Ferroptosis, necroptosis, and pyroptosis in the tumor microenvironment: Perspectives for immunotherapy of SCLC. *Semin. Cancer Biol.* 86 (3), 273–285. doi:10.1016/j.semcancer.2022.03.009

Pan, Y. M., Wang, C. G., Zhu, M., Xing, R., Cui, J. T., Li, W. M., et al. (2016). STAT3 signaling drives EZH2 transcriptional activation and mediates poor prognosis in gastric cancer. *Mol. Cancer* 15 (1), 79. doi:10.1186/s12943-016-0561-z

Paoli, P., Giannoni, E., and Chiarugi, P. (2013). Anoikis molecular pathways and its role in cancer progression. *Biochim. Biophys. Acta* 1833 (12), 3481–3498. doi:10.1016/j.bbamcr.2013.06.026

Peiris-Pages, M., Martinez-Outschoorn, U. E., Sotgia, F., and Lisanti, M. P. (2015). Metastasis and oxidative stress: Are antioxidants a metabolic driver of progression? *Cell Metab.* 22 (6), 956–958. doi:10.1016/j.cmet.2015.11.008

Ritchie, M. E., Phipson, B., Wu, D., Hu, Y., Law, C. W., Shi, W., et al. (2015). Limma powers differential expression analyses for RNA-sequencing and microarray studies. *Nucleic Acids Res.* 43 (7), e47. doi:10.1093/nar/gkv007

Rouillard, A. D., Gunderson, G. W., Fernandaz, N. F., Wang, Z., Monterio, C. D., McDermott, M. G., et al. (2016). *The harmonizome: A collection of processed datasets gathered to serve and mine knowledge about genes and proteins.* Oxford: Database.

Sakamoto, S., and Kyprianou, N. (2010). Targeting anoikis resistance in prostate cancer metastasis. *Mol. Asp. Med.* 31 (2), 205–214. doi:10.1016/j.mam.2010.02.001

Schumacker, P. T. (2015). Reactive oxygen species in cancer: A dance with the devil. *Cancer Cell* 27 (2), 156–157. doi:10.1016/j.ccell.2015.01.007

Sethi, N., and Kang, Y. (2011). Unravelling the complexity of metastasis - molecular understanding and targeted therapies. *Nat. Rev. Cancer* 11 (10), 735–748. doi:10.1038/nrc3125

Smith, A. D., Lu, C., Payne, D., Paschall, A. V., Klement, J. D., Redd, P. S., et al. (2020). Autocrine IL6-mediated activation of the STAT3-DNMT Axis silences the tnfα-RIP1 necroptosis pathway to sustain survival and accumulation of myeloid-derived suppressor cells. *Cancer Res.* 80 (15), 3145–3156. doi:10.1158/0008-5472.CAN-19-3670

Subramanian, A., Tamayo, P., Mootha, V. K., Mukherjee, S., Ebert, B. L., Gillette, M. A., et al. (2005). Gene set enrichment analysis: A knowledge-based approach for interpreting genome-wide expression profiles. *Proc. Natl. Acad. Sci. U. S. A.* 102 (43), 15545–15550. doi:10.1073/pnas.0506580102

Sundar, R., Huang, K. K., Kumar, V., Ramnarayanan, K., Demircioglu, D., Her, Z., et al. (2022). Epigenetic promoter alterations in GI tumour immune-editing and resistance to immune checkpoint inhibition. *Gut* 71 (7), 1277–1288. doi:10.1136/gutjnl-2021-324420

Sung, H., Ferlay, J., Siegel, R. L., Laversanne, M., Soerjomataram, I., Jemal, A., et al. (2021). Global cancer statistics 2020: GLOBOCAN estimates of incidence and mortality worldwide for 36 cancers in 185 countries. *Ca. Cancer J. Clin.* 71 (3), 209–249. doi:10.3322/caac.21660

Taddei, M. L., Giannoni, E., Fiaschi, T., and Chiarugi, P. (2012). Anoikis: An emerging hallmark in health and diseases. *J. Pathol.* 226 (2), 380–393. doi:10.1002/path.3000

Tang, C. T., Lin, X. L., Wu, S., Liang, Q., Yang, L., Gao, Y. J., et al. (2018). NOX4-driven ROS formation regulates proliferation and apoptosis of gastric cancer cells through the GLI1 pathway. *Cell. Signal.* 46, 52–63. doi:10.1016/j.cellsig.2018.02.007

Teng, F., Zhang, J. X., Chen, Y., Shen, X. D., Su, C., Guo, Y. J., et al. (2021). LncRNA NKX2-1-AS1 promotes tumor progression and angiogenesis via upregulation of SERPINE1 expression and activation of the VEGFR-2 signaling pathway in gastric cancer. *Mol. Oncol.* 15 (4), 1234–1255. doi:10.1002/1878-0261.12911

Vickers, A. J., and Elkin, E. B. (2006). Decision curve analysis: A novel method for evaluating prediction models. *Med. Decis. Mak.* 26 (6), 565–574. doi:10.1177/0272989X06295361

Vickers, A. J., Van Calster, B., and Steyerberg, E. W. (2016). Net benefit approaches to the evaluation of prediction models, molecular markers, and diagnostic tests. *BMJ* 352, i6. doi:10.1136/bmj.i6

Wang, K., Yuen, S. T., Xu, J., Lee, S. P., Yan, H. H. N., Shi, S. T., et al. (2014). Whole-genome sequencing and comprehensive molecular profiling identify new driver mutations in gastric cancer. *Nat. Genet.* 46 (6), 573–582. doi:10.1038/ng.2983

Wang, Y., Liu, X., Zhang, H., Sun, L., Zhou, Y., Jin, H., et al. (2014). Hypoxia-inducible lncRNA-AK058003 promotes gastric cancer metastasis by targeting gamma-synuclein. *Neoplasia* 16 (12), 1094–1106. doi:10.1016/j.neo.2014.10.008

Xu, G., Zhang, B., Ye, J., Cao, S., Shi, J., Zhao, Y., et al. (2019). Exosomal miRNA-139 in cancer-associated fibroblasts inhibits gastric cancer progression by repressing MMP11 expression. *Int. J. Biol. Sci.* 15 (11), 2320–2329. doi:10.7150/ijbs.33750

Yang, S. C., Wang, W. Y., Zhou, J. J., Wu, L., Zhang, M. J., Yang, Q. C., et al. (2022). Inhibition of DNMT1 potentiates antitumor immunity in oral squamous cell carcinoma. *Int. Immunopharmacol.* 111, 109113. doi:10.1016/j.intimp.2022.109113

Yarchoan, M., Hopkins, A., and Jaffee, E. M. (2017). Tumor mutational burden and response rate to PD-1 inhibition. *N. Engl. J. Med.* 377 (25), 2500–2501. doi:10.1056/NEJMc1713444

Ye, G., Yang, Q., Lei, X., Zhu, X., Li, F., He, J., et al. (2020). Nuclear MYH9-induced CTNNB1 transcription, targeted by staurosporin, promotes gastric cancer cell anoikis resistance and metastasis. *Theranostics* 10 (17), 7545–7560. doi:10.7150/thno.46001

Yu, H., and Jove, R. (2004). The STATs of cancer--new molecular targets come of age. *Nat. Rev. Cancer* 4 (2), 97–105. doi:10.1038/nrc1275

Yu, H., Pardoll, D., and Jove, R. (2009). STATs in cancer inflammation and immunity: A leading role for STAT3. *Nat. Rev. Cancer* 9 (11), 798–809. doi:10.1038/nrc2734

Zhang, T., Wang, B., Su, F., Gu, B., Xiang, L., Gao, L., et al. (2022). TCF7L2 promotes anoikis resistance and metastasis of gastric cancer by transcriptionally activating PLAUR. *Int. J. Biol. Sci.* 18 (11), 4560–4577. doi:10.7150/ijbs.69933

Zhang, Z., Han, S., Ouyang, S., Zeng, Z., Liu, Z., Sun, J., et al. (2022). PDK4 constitutes a novel prognostic biomarker and therapeutic target in gastric cancer. *Diagn. (Basel)* 12 (5), 1101. doi:10.3390/diagnostics12051101

Zhong, X. L., and Rescorla, F. J. (2012). Cell surface adhesion molecules and adhesion-initiated signaling: Understanding of anoikis resistance mechanisms and therapeutic opportunities. *Cell. Signal.* 24 (2), 393–401. doi:10.1016/j.cellsig.2011.10.005

Glossary

APC co_stimulation antigen-presenting cell co-inhibition
APC co_inhibition antigen-presenting cell co-inhibition
ARGPS anoikis-related gene prognostic score
ARGs anoikis-related genes
AUC area under the ROC curve
CCR C-C chemokine receptor
DEGs differentially expressed genes
DNMT1 DNA methyltransferase 1
EZH2 enhancer of zeste homologue 2
EMT epithelial–mesenchymal transition
exp expression
GC gastric cancer
GEO Gene Expression Omnibus
GSEA Gene Set Enrichment Analysis
GLI1 GLI family zinc finger 1
GO Gene Ontology
HLA human lymphocyte antigen
IL-6 interleukin-6
IGF-1 insulin-like growth factors-1
lncRNA long non-coding RNA
JAK Janus tyrosine Kinase
KM Kaplan-Meier
LASSO least absolute shrinkage and selection operator
MMP11 matrix metalloproteinase 11
NOX4 NADPH oxidase 4
MDSC Myeloid-derived suppressor cells
MHC_class_I major histocompatibility complex class I
NCBI National Center for Biotechnology Information
OS overall survival
PCNA proliferating cell nuclear antigen
PDK4 pyruvate dehydrogenase kinase-4
ROC receiver operating characteristic
ROS reactive oxygen species
STAD stomach adenocarcinoma
TCGA The Cancer Genome Atlas
ssGSEA Single-sample Gene Set Enrichment Analysis
TMB tumor mutation burden
SKP2 s-phase kinase associated protein 2
PDGFRB platelet derived growth factor receptor Beta
SERPINE1 serine protease inhibitor clade E member 1
SNCG γ-synuclein
STAT3 signal transducer and activator of transcription 6
THY1 Thy-1 cell surface antigen
Type_I_IFN_Reponse type I interferon response
Type_II_IFN_Reponse type II interferon response
VEGF vascular endothelial growth factor.